Journal of Applied Mechanics and Technical Physics, Vol. 37, No. 4, 1996

ANOMALOUS TWO-LAYER FLOW REGIMES OVER AN OBSTACLE

N. V. Gavrilov and V. Yu. Liapidevskii

UDC 532.539.2; 532.52

1. Introduction. In this paper, we study the structure of long waves generated by a two-dimensional obstacle at the bottom in shift, two-layer flow of an immiscible fluid. The formation and propagation of finite-amplitude disturbances in flows, particularly in supercritical flows over an obstacle, is an essentially nonlinear process which is affected by many physical factors such as the interaction of fluids at the interface, wall effects, viscosity, surface tension, etc. The aim of this work is to elucidate the possibility of using the simplest two-layer flow model in a shallow water approximation for qualitative and quantitative description of various flow regimes in a two-dimensional channel with an uneven bottom.

It is well known [1–3] that in one-layer flow over fairly extended bottom irregularities, the flow is either disturbed locally or subcritical upstream flow becomes supercritical downstream flow, while the flow above the crest is critical. In such a regular flow regime, the obstacle completely controls the upstream flow. In a two-layer stratified fluid, new flow regimes over an obstacle occur in which the obstacle supports the propagation of nonlinear perturbations. At the same time, the flow above the crest of the obstacle is completely supercritical and a change in the obstacle height does not influence the upstream flow. Such anomalous two-layer flows for a water–kerosene system were found experimentally by Long and Baines [1, 2], and Lawrence [3, 4] has studied such flows for miscible liquids. Baines [2] has given a detailed description of possible flow regimes and made a comparison with experiments on the motion of an obstacle at a constant velocity in a two-layer fluid at rest. This problem was solved numerically by Houghton and Isaacson [5]. The flow of a two-layer miscible fluid over an immovable obstacle without a velocity shift between the layers has been studied experimentally by Lawrence [3, 4]. A thorough review of works on the influence of topography on the structure of stratified flows in the atmosphere and the ocean is given by Baines [6].

The majority of investigations of the structure of long waves above an obstacle are devoted to stationary problems. A nonstationary approach to the problem of generation of long waves by an obstacle has been used by Baines and Liapidevskii [2, 7]. Liapidevskii [7] formulated the generalized Riemann problem and plotted regular flow diagrams in the plane of the determining problem parameters for the equations of two-layer shallow water in the Boussinesq approximation. In this case, in contrast to [2], an initial shift between the layers in undisturbed flow was assumed. An analysis of stationary solutions in [7] and also numerical solutions of the nonstationary problem have shown that the occurrence of an internal hydraulic jump (more precisely, "drop") on the lee side of an obstacle in anomalous flow regimes is due to the nonmonotonic dependence of flow parameters on the obstacle height rather than to the influence of downstream conditions, as was assumed in [2, 3].

In this work, we studied experimentally the possibility of realizing completely supercritical asymmetric flow regimes over an obstacle placed in uniform flow of an immiscible two-layer fluid with an initial velocity shift between the layers. We studied the flow parameters for which finite-amplitude perturbations either cannot propagate upstream from the obstacle or their velocity is very low. This makes it possible to study transition of the flow to a stationary regime and also to compare experimental and numerical results.

Lavrent'ev Institute of Hydrodynamics, Siberian Division, Russian Academy of Sciences, Novosibirsk 630090. Translated from Prikladnaya Mekhanika i Tekhnicheskaya Fizika, Vol. 37, No. 4, pp. 81–88, July–August, 1996. Original article submitted January 11, 1995; revision submitted May 23, 1995.

0021-8944/96/3704-0527 $15.00

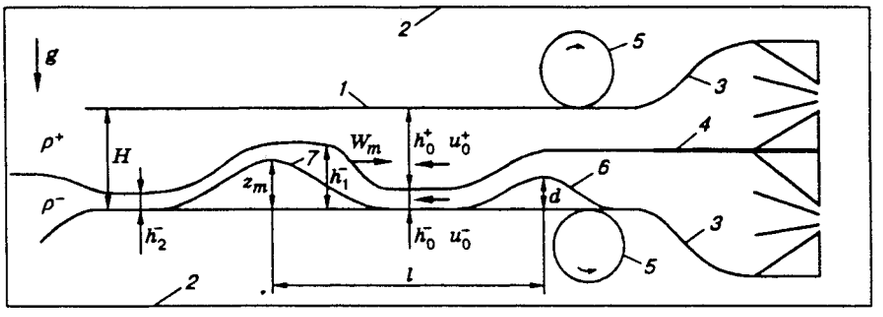

Fig. 1

2. Two-Layer Shallow Water Equations. In the Boussinesq approximation $[(\rho^- - \rho^+)/\rho^+ \ll 1]$ the equations of plane–parallel two-layer flow over an uneven bottom have the form

$$h_t^+ + (h^+u^+)_x = 0, \quad h_t^- + (h^-u^-)_x = 0, \quad u_t^+ + \left(\frac{1}{2}(u^+)^2 + \frac{1}{\rho^+}p^+\right)_x = 0,$$
$$u_t^- + \left(\frac{1}{2}(u^-)^2 + b(h^- + z) + \frac{1}{\rho^+}p^+\right)_x = 0, \qquad h^+ + h^- + z = H \equiv \text{const}. \tag{2.1}$$

Here $h^\pm$, $\rho^\pm$, and $u^\pm$ are the thickness, densities, and horizontal velocities of the upper and lower layers; p^+ is the pressure on the upper boundary of the flow; H is the total channel depth; $b = (\rho^- - \rho^+)g/\rho^+$ is the buoyancy; g is the acceleration of gravity; $z = z(t,x)$ is the location of the channel bottom. The Boussinesq approximation allows one to filter out surface waves and to considerably simplify the model. Therefore, Eq. (2.1) will be used to describe the water–kerosene system, although the relation $(\rho^- - \rho^+)/\rho^+ \simeq 0.25$ cannot be considered small. It is known that the problem of choice of relations at internal hydraulic jumps cannot be solved uniquely within the framework of a two-layer model. Therefore, we use relations that follow from the divergent form of Eq. (2.1). These equations are the limiting case of equations derived in [8] for two-layer flow with allowance for small-scale flow at the interface between the layers, in which the thickness of the interlayer between the homogeneous layers tends to zero.

The structure of self-simular solutions of the Riemann problem for $z \equiv 0$ has been studied by Armi [9]. If the channel bottom is not flat $[z(t,x) \not\equiv 0]$, the problem of nonstationary flow in the channel does not have self-similar solutions. However, for a fixed localized obstacle and constant parameters of incoming flow, the solution of system (2.1) for large times becomes self-similar. In this case, a near-steady flow regime is realized over the obstacle. This circumstance was used in [2, 7] to formulate the problem of two-layer flow over an obstacle in the class of self-similar solutions.

Let us assume for definiteness that two layers move uniformly in one direction at a velocity $u_0^\pm < 0$ (Fig. 1). At $t = 0$, the bottom in the vicinity of the point $x = 0$ suddenly takes the shape of a blunt obstacle, as shown in Fig. 1. Then, a finite-amplitude disturbance will propagate upstream ($x > 0$) and at a sufficient distance from the obstacle this disturbance becomes a combination of an internal bore followed by a simple elevation wave [7]. For a relatively small dimension of the obstacle, we can assume that the wave is centered at the point (0,0), i.e., we shall seek a self-simular solution of system (2.1) that depends only on the variable $\xi = x/t$. The flow over the obstacle is steady, and, by virtue of (2.1), the following relations hold:

$$h^+u^+ = h_1^+u_1^+ = Q^+, \quad h^-u^- = h_1^-u_1^- = Q^-, \quad \frac{1}{2}u^{+2} + \frac{1}{\rho^+}p^+ = \frac{1}{2}u_1^{+2} + \frac{1}{\rho^+}p_1^+ = J^+,$$
$$\frac{1}{2}u^{-2} + b(h^- + z) + \frac{1}{\rho^+}p^+ = \frac{1}{2}u_1^{-2} + bh_1^- + \frac{1}{\rho^+}p_1^+ = J^-, \tag{2.2}$$

where the subscript 1 denotes the flow state upstream the obstacle. Note that relations (2.2) coincide with those used in [9] for analysis of steady two-layer flows over an obstacle. The flow regime is called regular if

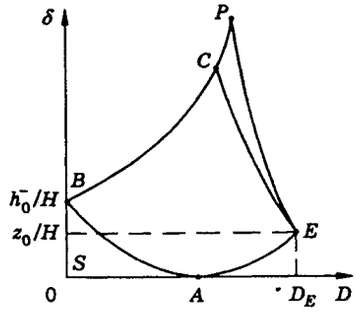

Fig. 2

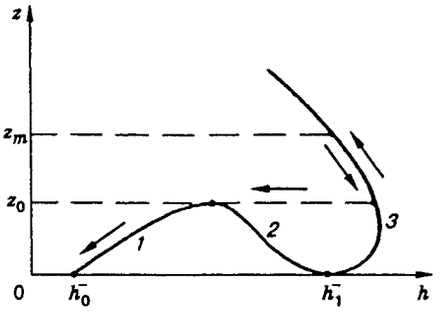

Fig. 3

there is a continuous solution of (2.2) that relates subcritical state 1 to supercritical state 2. This is possible only if the flow above the crest of the obstacle is critical, i.e., if $z = z_m = \max z(x)$:

$$\Delta = \frac{u^{-2}}{bh^-} + \frac{u^{+2}}{bh^+} - 1 = 0. \tag{2.3}$$

In this case, $\Delta_1 < 0$ in front of the obstacle, and $\Delta_2 > 0$ behind it. Conditions (2.2) and (2.3) for a given value of z_m give an additional relation between h_1^- and u_1^-, which is required to find a self-similar solution in the region $x > 0$. The solution is completely determined by the dimensionless parameters $\alpha = h_0^-/H$, $\gamma = (u_0^- - u_0^+)/\sqrt{bH}$, $D = -u_0^-/\sqrt{bH}$, and $\delta = z_m/H$.

For fixed values of α and γ, the region of regular solutions can be found in the plane of the parameters (D, δ) [7]. For $\alpha = 0.15$ and $\gamma = -0.18$ region $ASBPE$ is shown in Fig. 2. Curve PB corresponds to the completely blocked flow of the lower layer ($u_1^- = 0$, $\delta = h_0^-/H$). In region ABS, a centered rarefied wave propagates ahead of the obstacle. Region $ABCE$ corresponds to flow with an internal bore which propagates upstream at velocity $W > 0$. In curve AE, the bore has velocity $W = 0$. The values of the parameters on curve CE ensure the propagation of a bore of maximum amplitude at velocity $W_m > 0$. The propagation velocity of nonlinear disturbances W_m is maximal for this system. In region PCE, a simple centered wave is adjacent to the bore of maximal amplitude. The left-hand boundary of this wave reaches the obstacle on curve PE, and the flow ahead of the obstacle becomes critical. A further increase in obstacle height does not change the upstream flow pattern. Therefore, above curve PE the regular flow regime is impossible. Beneath curve AE, all perturbations move downstream and completely supercritical flow is established over the obstacle.

The most interesting point in the $D - \delta$ diagram is point E to which several regions with different flow regimes are adjacent. In this case, no long-wave finite-amplitude perturbations with $D > D_E$ can propagate upstream and for an obstacle of any height the flow pattern is nearly steady. For this reason, the vicinity of point E was investigated experimentally.

Let $D = D_E$. Then the relation $z = z(h)$ ($h = h^-$) obtained from (2.2) takes the form shown in Fig. 3. Branches (1) and (3) correspond to supercritical flow ($\Delta > 0$) and branch (2) to subcritical flow over the obstacle ($\Delta < 0$). If $z_m < z_0$, a symmetric supercritical flow regime along branch (1) is realized. For $z_m > z_0$, a stationary hydraulic jump ($W_m = 0$), which converts the flow to state 1, forms ahead of the obstacle, and lift of the flow at height z_m is possible only along branch (3). In principle, the flow can return along the same branch to state 1 behind the obstacle. This flow regime, however, does not occur, as is seen from experiments and numerical solutions of the nonstationary problem. The flow denoted by arrows in Fig. 3 is more stable. The flow rises along supercritical branch (3) to the level $z = z_m$ on the front slope and descends symmetrically to the level $z = z_0$ on the back slope. Then follows a hydraulic jump (more precisely, "drop"), which changes the flow to critical flow in curve (1), and, finally, acceleration along curve (1) to the initial critical state 0 takes place.

Note that according to system (2.1), in stationary hydraulic jumps, the energy in each layer is conserved. Therefore, the occurrence of an internal hydraulic jump on the leeward slope is not associated with the loss

of energy due to mixing, etc., as was assumed by Baines [2]. Moreover, the solution constructed converts the critical state ahead of the obstacle to the same state behind the obstacle. Thus, downstream conditions also should not influence the flow structure, as is stated by Lawrence [3], provided the supercritical downstream flow regime is ensured.

An asymmetric supercritical flow regime is realized experimentally on a setup described in the next section. Note also that for $z_m = z_0$ and $D = D_E$ three different steady flow regimes near the obstacle are possible, because regions of regular, anomalous, and supercritical regimes are adjacent to point E. All these flows are realized numerically in [7].

3. Experiment. Experiments were conducted on an experimental setup of a closed type 2220 cm long, 15 cm wide, and 40 cm high, whose working channel (1) 120 cm long with height $H = 6$ cm has a rigid horizontal bottom and a lead (see Fig. 1). The setup incorporates return channels (2), turning devices with smooth entrances (3), and a separating wall (4). Fluids are caused to flow by means of original plungers (5), which are cylinders rotating about their axis and located asymmetrically between the bottom and the lead of the return channels [10]. A blunt obstacle (6) 20 cm long with a varied height d was located at the entrance of the working channel to generate controlled supercritical flow.

Wave generation at the interface was performed by means of a flexible brass plate 7 0.2 mm thick, whose upstream end was fixed rigidly and the opposite end of which can move only in the horizontal direction. The plate in the initial state does not extend above the bottom of the working channel. In addition a special device could bend the plate so that a blunt obstacle appears on the channel bottom. The shape of this obstacle is well approximated by a fourth-order curve. The obstacle (7) length was 40 cm and the height z_m was varied form 0 to 3.5 cm. The center of the obstacle was located at distance $l = 45$ cm from the center of the obstacle 6. Water with density $\rho^- = 1$ g/cm^3 and kerosene with $\rho^+ = 0.8$ g/cm^3 were used as the working fluids.

The layer velocities in the working channel were determined as in [10]. Using camera recording, we measured the velocity profiles and flow rates in the return channels and then used these profiles to calculate the flow-rate-averaged layer velocities u^+ and u^-. In addition, in some experiments we measured, for reference, the velocities immediately in the working channel. For this, by means of a stop-watch, we detected repeatedly the time required for a solid particle of neutral buoyancy to travel the reference region of the channel. The time was then averaged and the average flow velocities in each of the layers were determined. Both methods gave similar results and the velocity measurement error did not exceed 8%.

The location of the interface between the layers was determined by camera recording of a luminous screen through the bulk of the liquid. Since the liquids were immiscible, the interface is clearly seen in the photograph. Therefore we need neither color the layers nor shade the details of the wave pattern occurring at the interface between the layers. The error in determining dimensions by photographs did not exceed 5%.

The experimental and calculated data were compared. The main difficulty in comparing was that ideal fluids were considered in the model. Viscosity leads to flow nonuniformity along the channel. For partial compensation of this effect, the flume was positioned with a small slope (1 : 80) so that in the absence of an obstacle the flow along the entire working region remains supercritical and nearly uniform.

Figures 4 and 5 give a comparison of the experimental and calculation results for two-layer shift flow over an obstacle for $D \simeq D_E$. For a more instructive illustration, the horizontal dimension is reduced twice in comparison with the vertical dimension. The solid curves are the interface obtained in the experiments and the dashed curves are the numerical solution of the problem of placement of an obstacle into uniform flow within the framework of model (2.1). The arrows show the direction of motion of the layers. In the calculations we used a scheme similar to the scheme of S. K. Godunov without separation of discontinuities. A modification of the right-hand side of Eqs. (2.1) due to allowance for the slope and friction on the channel walls brings about no significant changes in the numerical solution.

Figure 4 illustrates the case of flow with a significant initial shift between the layers ($u_0^+ \simeq -12$ cm/sec, $u_0^- \simeq -29$ cm/sec, $h_0^- = 1.2$ cm). The theoretical and experimental boundaries D_E of the steady flow regimes coincides within the measurement accuracy. Due to a decrease of about 0.5 cm/sec in the layer velocities, the steady flow regime (Fig. 4a) becomes unsteady (Fig. 4b). A bore of maximum amplitude departs from the obstacle and then propagates upstream at a low velocity. A decrease of from 3.4 cm (Figs. 4a and 4b) to

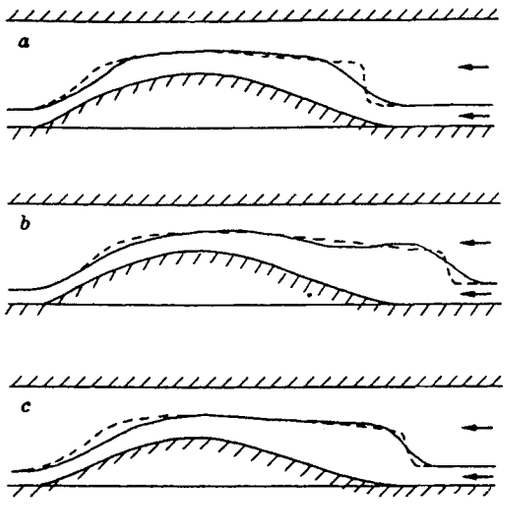

Fig. 4

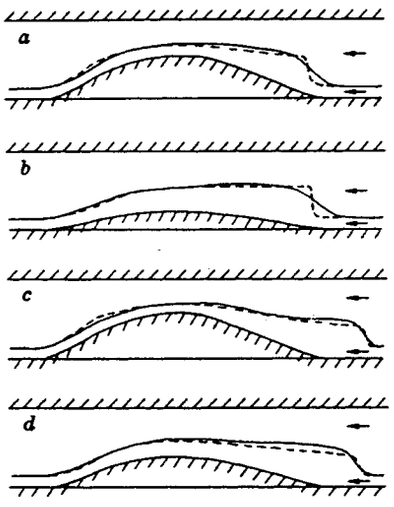

Fig. 5

3 cm (Fig. 4c) in obstacle height z_m does not influence bore propagation. In the plane (D, δ) (see Fig. 2) this means that $D = D_E$ for Fig. 4a and $D < D_E$ for Figs. 4b and 4c, and in all three cases the anomalous flow regime shown by the arrows in Fig. 3 is realized above the obstacle. Of course, hydraulic jumps, which are modeled in (2.1) by discontinuities, cover a substantial region above the obstacle in numerical solution and experiment. In real flow in the region of a hydraulic jump the assumption of hydrostatic-pressure distribution in the layers is violated, and in smearing the numerical solution depends on the properties of the diagram. Therefore, in the vicinity of hydraulic jumps on the frontal and back slopes of the obstacle, a discrepancy between the numerical and experimental data is observed. Nevertheless it can be argued that Eqs. (2.1) of shallow water describes both qualitatively and quantitatively the anomalous flow regimes over an obstacle. Consequently, asymmetric supercritical flows are stable against unsteady one-dimensional perturbations, and symmetric flows are unstable, although the latter statement should be regarded as an experimental rather than theoretical fact. Note that the second approximation of the equations of shallow water theory should be used to describe more adequately the inner bore, but in this case the corresponding analytical solutions and flow diagrams cannot be constructed.

Another phenomenon in model (2.1) that was not taken into account is generation of short waves at the interface under the action of the velocity shift between the layers. To estimate the effect of this fact on the two-layer flow structure in a series of experiments whose data are given in Fig. 5, the difference in velocity between the layers is considerably decreased ($u_0^+ \simeq -17$ cm/sec, $u_0^- \simeq -24$ cm/sec and $h_0^- = 0.9$ cm), although the upstream flow parameters were so that $D \simeq D_E$. In this case, the experimental and numerical results agree much better. This is explained, on the one hand, by the similarity between real flow and the two-layer model using (2.1) and, on the other hand, by the fact that the amplitude of the jumps on the leeward slope of the obstacle decreases with decreasing difference in velocity. Figure 5 illustrates the influence of the obstacle on the anomalous flow structure. Significant changes in the height of the obstacle $z_m \simeq 3.2$, 1.5, 3.5, and 2.3 cm (Figs. 5a–5d) do not change the flow structure. At the same time, a change in the incoming flow velocity only by several percent changes abruptly the upstream flow [transition from steady (Figs. 5a and 5b) to unsteady flow (Figs. 5c and 5d)].

4. Conclusion. A comparison of the experimental and numerical data shows that for immiscible fluids the instability of symmetric supercritical flow over an obstacle can be established using the simplest model of two-layer flow (2.1) ignoring the effects of interaction of fluids with rigid interfaces and at the interfaces.

Modeling of two-layer flows of miscible fluids involves study of the mutual influence of the obstacle and mixing on the blocking effects of the flow and can be only performed using a more complex model [11]. It has

been shown [11] that, as a result of mixing, a blocked zone of finite length forms upstream of the obstacle. At large Froude numbers of the incoming flow, the mixing region can completely overlap one of the layers, and the flow diagram in Fig. 2 will differ considerably from the real flow pattern.

This work was partially supported by the Russian Foundation for Fundamental Research (Grant 94-01-01210-a).

REFERENCES

1. R. R. Long, "Some aspects of the flow of stratified fluids. II. Experiments with a two-fluid system," *Tellus*, **6**, 97–115 (1954).
2. P. G. Baines, "A unified description of two-layer flow over topography," *J. Fluid Mech.*, **146**, 127–167 (1984).
3. G. A. Lawrence, The Hydraulics and Mixing of Two-Layer Flow over an Obstacle, PhD thesis, Department of Civil Engineering, University of California, Berkeley (1985).
4. G. A. Lawrence, "The hydraulics of steady two-layer flow over an obstacle," *J. Fluid Mech.*, **254**, 605–633 (1993).
5. D. D. Houghton, E. Isaacson, "Mountain winds," *Stud. Numer. Anal.*, **2**, 21–52 (1970).
6. P. G. Baines, "Upstream blocking and airflow over mountains," *Ann. Rev. Fluid Mech.*, **19**, 75–97 (1987).
7. V. Yu. Liapidevskii, "Generation of long waves by the bottom topography in a two-layer flow," *Prikl. Mekh. Tekh. Fiz.*, **35**, No. 3, 34–47 (1994).
8. V. Yu. Liapidevskii, "Model of two-layer shallow water with an irregular interface," in: *Laboratory Modeling of Dynamic Processes in the Ocean* [in Russian], Inst. of Thermal Physics, Sib. Div., Russian Acad. of Sci., Novosibirsk, 87–97 (1991).
9. L. Armi, "The hydraulics of two flowing layers with different densities," *J. Fluid Mech*, **163**, 27–58 (1986).
10. N. V. Gavrilov, "Internal solitary waves and smooth bores which are stationary in a laboratory coordinate system," *Prikl. Mekh. Tekh. Fiz.*, **35**, No. 1, 29–34 (1994).
11. V. Yu. Liapidevskii, " Blocking effects in a two-layer flow of an immiscible fluid over an obstacle," *Prikl. Mat. Mekh.*, **58**, No. 4, 108–112 (1994).